

DESIGN AND FLUID-SOLID-HEAT COUPLING ANALYSIS OF AN ELECTROSTATIC DEFLECTOR FOR HUST SCC250 PROTON THERAPY FACILITY

S. W. Hu, L. G. Zhang, Z. Y. Mei, Z. J. Zeng, X. F. Li, K. J. Fan†

Institute of Applied Electromagnetic Engineering, Huazhong University of Science and Technology, Wuhan, China

Abstract

The study of proton therapy equipment has earned more and more attention in recent years in China. A superconducting cyclotron based proton therapy facility is being developed for/at Huazhong University of Science and Technology (HUST). The proton beam is extracted by means of electrostatic deflectors followed by a series of magnetic channels. This paper introduces the design of an electrostatic deflector, including the structure optimization and the material selections. In order to minimize the risk of destruction caused by the proton beam loss, fluid-solid-heat coupling analysis for the deflector has been conducted by applying computational fluid dynamics (CFD) on ANSYS 16.0 software. The maximum temperatures of the septum in various cases of cooling water speed, septum thickness and material have been investigated respectively. The result based on thermal analysis will give us a valuable reference to choose a suitable configuration for the deflector.

INTRODUCTION

Proton therapy is becoming one of the dominant methods for cancer treatment since proton beam provides a superior dose distribution in several anatomic sites [1]. Much endeavour has been made to grow key technologies of proton therapy in China in recent years. In this context, a superconducting cyclotron based proton therapy facility is being developed at Huazhong University of Science and Technology. The extracting proton beam energy is designed to be 250MeV and the beam current is above 800nA. The proton beam is exacted by precessional exaction method that is accomplished by bump coils, electrostatic deflectors (ESD) and passive magnetic channels (MC). A schematic view of our extraction system is shown in Figure 1.

In a cyclotron, the turn separation is inversely proportional to the radius [2]. The beam might stack up in the extraction radius owing to the extremely small turn separation. It is exceedingly difficult for ESD to peels off the last turn without affecting the inner turns and with much less beam loss. Therefore, the septum thickness must be small enough regularly ranging from 0.1-1mm. The deposited beam energy is a risk of destruction for ESD and its performance directly influences the beam parameters.

Based on above, this paper mainly presents the discussion about the structure design and fluid-solid-heat coupling analysis for the electrostatic deflector and dedicates to providing valuable reference to its configuration.

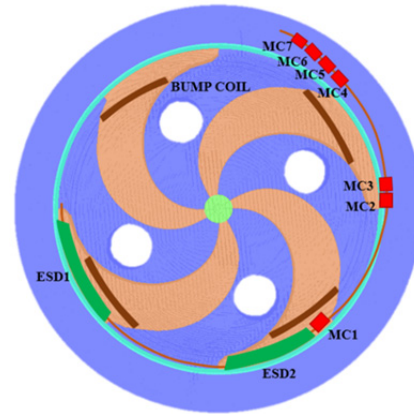


Figure 1: Layout of HUST SCC250 extraction system.

DESIGN AND CONSIDERATIONS

The beam loss rate at the first deflector is assumed to be 60%, which means the deposited energy on the septum is 120W. As the electrode is charged with -60KV high voltage, we also care about the sparking phenomenon in the vacuum chamber. Thus in order to reduce the impact brought by the thermal effect and sparking phenomenon, we focused on the structure optimization and material selections of the deflector. Figure 2 presents the main structure of our designed deflector.

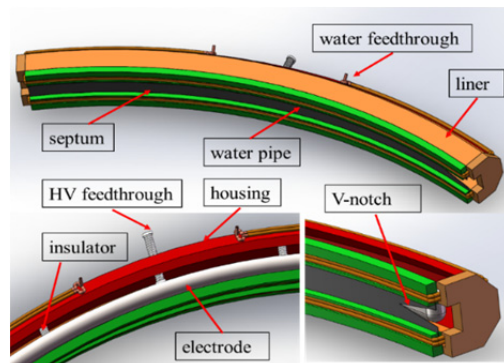


Figure 2: Main structure of the designed deflector.

Several aspects are taken into consideration as following:

- (1) The cooling water pipes are placed in the trenches to make the forced convection heat exchange more effective.
- (2) A V-notch is designed in the leading edge of the septum in order to expand the thermal region where the beam deposits the energy.

† kjfan@hust.edu.cn

(3) It has been found that all the materials constituent the electrostatic deflector give significant contributions to the mechanism of breakdown [3]. The material selections of some parts have been tabulated in Table 1

Table 1: Material Selections of Some Parts

| Part | Material |
|---------------|-------------------------|
| Electrode | Hard-anodized aluminium |
| Liner/Housing | OFHC |
| Septum | Tungsten |
| Insulator | AlN ceramic |

THERMAL MODEL

The fluid-solid-heat coupling analysis of the deflector is conducted by CFX module in the FEA software ANSYS 16.0. Most of the beam losses occur at the entrance edge of the deflector thus the heat mainly gathers in the leading region [4]. To simply the calculation, we choose 1/4 length part of the overall deflector to be the basic thermal model. The thermal model shown in figure 3.

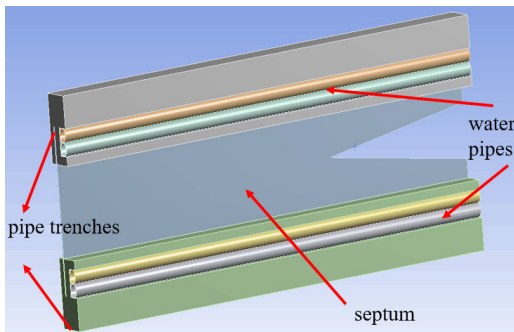


Figure 3: Thermal model of the deflector in CFX.

Conditions of Calculations

The distribution of the power intensity Q on the septum can be nearly regarded as Gaussian distribution and surface heat source. The following relation expresses the Gaussian distribution in one dimension

$$Q(x) = Q_0 \exp\left(-\frac{x^2}{2\sigma^2}\right) \quad (1)$$

Q_0 is constant. The value of σ depends on the beam size, for this thermal model in the calculation, $\sigma = 3mm$ calculated by beam dynamics. Actually when the deflector is operating, the phase space of the beam and the position of the deflector vary from time to time, so the distribution region of beam loss is irregular. This condition is dealt with in an extreme way--all the deposited power is imposed on the lateral sides of the V-notch distributing along the edge at a length of 12mm.

The total thermal power P is calculated as follows:

$$P = \int Q * S ds = \sum_{i=1}^n Q(i)S(i) = \sum_{i=1}^n Q(i) * \Delta l(i) * \delta \quad (2)$$

Where $i=0,1,...,11$, $\Delta l(i)=1mm$, δ is the thickness of the septum. For this simulation, $\delta=3mm$, $P=120W$.

Figure 4 presents the discrete input heat flux derived from Gaussian distribution.

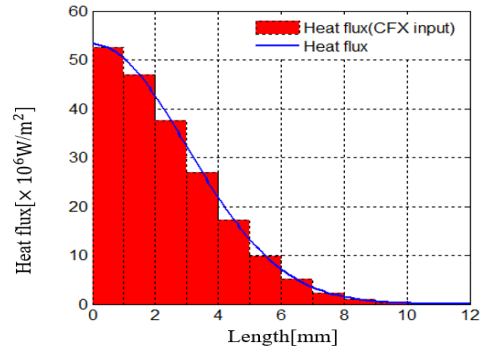


Figure 4: Input heat flux on the lateral surface of the septum.

For the boundary condition at the inlet, uniform temperature is 20° C and uniform water flow speed is 0.2m/s. At the outlet, the 0Pa average static pressure is applied. The wall condition is set to be no slip, adiabatic. The cooling water in four water pipes all flows to the same direction. The k-epsilon turbulent model is chosen in this analysis. When the turbulence kinetic energy and heat transfer falls below 10^{-4} , the calculation is considered to be convergent.

RESULTS AND DISCUSSION

Figure 5 shows the temperature field of the model, in the case that the thickness of tungsten septum is 0.3mm, the cooling water flow speed at inlet is 0.2m/s and the beam loss power is 120W. The maximum temperature of the septum reaches up to around 1324K, which appears in the central zone of the input heat flux--the V-notch corner edge.

We can also get the contour graph of structural deformation distribution [5] from the following figure 6, The expansion of the material produced a bulging that is about 0.0268mm.

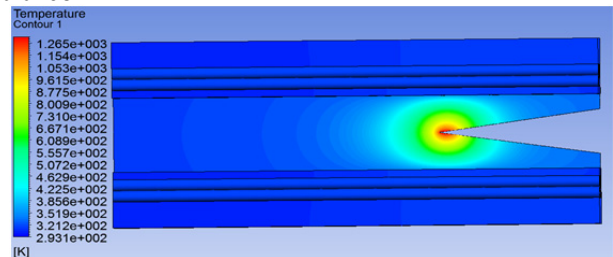


Figure 5: Temperature field of the thermal model.

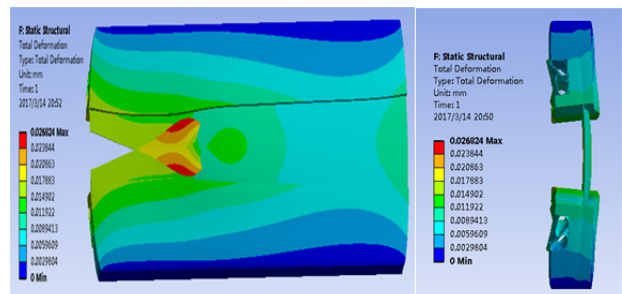


Figure 6: Structural deformation of the overall deflector model.

Cooling Water Flow Speed

Increasing the water flow speed can enforce the thermal exchange rate. However, the fluid resistance in the pipe is proportion to the square of the flow speed. As the resistance increases, the state of the water flowing may change. Figure 7 indicates the maximum temperatures on the septum at various water flow speeds.

Figure 7 tells that the maximum temperature decreases with the water flow speed rises from 0.2m/s to 6m/s, but the rate of temperature decrease falls consequently. It's suggested that the water flow speed should be set at about 0.5-1m/s taking into account the power consumption of water pumps/

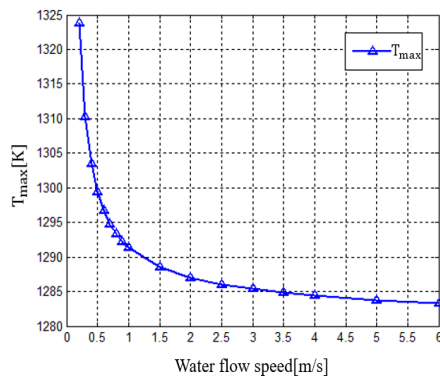


Figure 7: Maximum temperature on the septum at different water flow speeds.

Thickness of the Septum

Thinner septum produces less beam loss when the gap between septum and electrode is fixed. Meanwhile the thickness influences the heat transfer on the septum. The influence that the thickness of the septum exerts to thermal diffusion is sophisticated. The maximum temperature and the maximum displacement of the septum as a function of thickness, in the case of the input heat flux in figure 4, are shown in figure 8.

As figure 8 shows, the maximum displacement almost increases linearly with the septum thickness and it is closely related to the input power at various thickness. The maximum temperature at 0.35mm thickness is higher than the 0.40mm thickness is that perhaps thermal diffusion increases more than the input thermal power does.

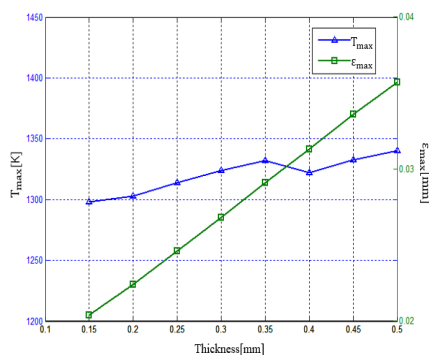


Figure 8: Calculated maximum temperature and displacement as a function of thickness.

Material of the Septum

The septum is expected to have relatively high melting point and heat transfer coefficient. Table 2 gives a summary of some simulating results obtained with several common septum materials. The thickness is 0.3mm and heat power is up to 120W.

Table 2: A List of Simulating Results for Four Materials

| Material | Melting point (K) | Thermal conductivity (W/(mk)) | Maximum temperature (K) | Maximum deformation (mm) |
|---------------------|-------------------|-------------------------------|-------------------------|--------------------------|
| 304 Stainless steel | ~1713 | 12.1 | 4786.2 | 0.1832 |
| Ta | 3290 | 57.5 | 3583.3 | 0.1076 |
| Mo | 2890 | 138 | 1572.1 | 0.0322 |
| W | 3695 | 173 | 1323.8 | 0.0268 |

Perhaps stainless steel is the most unsuitable one among the simulating materials, since it should have been melted at 4786.2K for its 1713K melting point. W seems to be the best material for the septum for its comparatively low temperature and tiny displacement.

CONCLUSION

This paper presents the structure design for the deflector with cooling water pipes. A thermal model is used to estimate the performance of the deflector based on fluid-solid-thermal analysis. The simulating results indicate that the maximum temperature is less than 1400K and the deformation is not serious for a W septum with a thickness of 0.3mm. It is essential to mention that in the simulation, the septum is postulated to be heated in an extreme way, the thermal model is simplified for easy calculation and radiation is also exempted from simulation. All these considerations above predict a conservative simulating result. Actually our simulating results should/will be compared with experimental results in the near future.

ACKNOWLEDGEMENT

This work was supported by the National Program for Research and Development of Digital Diagnostic Equipment Project under Grant 2016YFC0105303 through the Ministry of Science and Technology, China.

REFERENCES

- [1] W. Wieszczycka and W. H. Scharf, *Proton radiotherapy accelerators*, world scientific, 2001.
- [2] W. Kleeven, "Injection and extraction for cyclotrons", (2006).
- [3] M. Re, G. Cuttone, E. Zappala, S. Passarello, "Breakdown mechanisms in electrostatic deflector", in *Proc. AIP2001*, Ed. Felix Marti. Vol. 600. No. 1. AIP, 2001.
- [4] J. DeKamp and F. Marti, "Thermomechanical calculations of a cyclotron deflector", in *Proc. PAC97, 1997*. Vol. 1. IEEE, 1997.
- [5] ANSYS, 2014, User's Guide version 16.0.0, ANSYS Ltd.